MIC2021
21st Machining Innovations Conference for Aerospace Industry

Proceedings are available on SSRN: www.ssrn.com

SSRN Proceedings Hosted on SSRN.com

MIC Procedia (2021) 070–077

21st Machining Innovations Conference for Aerospace Industry 2021 (MIC 2021), December 1st and 2nd 2021, Hannover, Germany

Wear development of self-lubricating CrAlVN coatings during turning Ti6Al4V

Kirsten Bobzin [a], Christian Kalscheuer [a], Marco Carlet [a], Nina Stachowski [a *], Wolfgang Hintze [b], Carsten Möller [b], Petter Ploog [b]

[a]*Surface Engineering Institute (IOT), RWTH Aachen University, Kackertstraße 15, 52072 Aachen, Germany*
[b]*Institute of Production Management and Technology (IPMT), Hamburg University of Technology (TUHH), Denickestr. 17, 21073 Hamburg, Germany*

* Corresponding author. Tel.: +49 241 80 99368; fax: +49 241 80 92941. *E-mail address:* stachowski@iot.rwth-aachen.de

Abstract

Interactions between cutting tool and workpiece material are crucial to tool wear at the cutting edge. In particular difficult to machine materials like the titanium alloy Ti6Al4V require tailored solutions to avoid extensive tool wear. Temperature-active, self-lubricating chromium-aluminium-vanadium-nitride (CrAlVN) coatings deposited by physical vapor deposition (PVD) have shown the potential to reduce tool wear during Ti6Al4V turning. These coatings form lubricating oxide phases at temperatures between 700 °C ≤ ϑ ≤ 800 °C which might be suitable to reduce thermal and mechanical loads during cutting. However, the initial wear development as well as the formation of lubricating oxide phases during Ti6Al4V turning while using cooling lubricant have not been adequately investigated. Consequentially, it is unclear whether the lubricating oxide phases form during the turning operation with flood cooling. Nevertheless, this is of interest, because the use of cooling lubricant is state of the art in turning of Ti6Al4V in order to reach an increased tool life. That is why, the initial tool wear within the first two minutes of turning with flood cooling was investigated in this study. For this purpose, two different CrAlVN coatings with varying V/Al ratios were deposited on cemented carbide inserts by a hybrid direct current magnetron sputtering (dcMS) / high power pulsed magnetron sputtering (HPPMS) process using an industrial coating unit. Subsequently, cutting tests with a depth of cut a_p = 1.2 mm, feed rate f = 0.12 mm, setting angle κ_r = 95° and cutting velocity v_c = 80 m/min were conducted at defined cutting intervals of t_c = 5 s, 10 s, 20 s, 40 s, 80 s and 120 s using a computer numerical controlled (CNC) lathe machine. The initial tool wear development, prevailing wear mechanisms as well as the formed oxide phases during the intervals were analyzed. Uncoated cemented carbide inserts were used as a reference. The results highlight that the formation of lubricating vanadium oxides is possible in turning process with cooling lubricant. Furthermore, it seems that adhesion processes are the main causes of tool failure. The results offer the possibility to adapt the CrAlVN coatings for Ti6Al4V turning.

Keywords: Tool coatings; PVD; self-lubrication; turning; Ti6Al4V

1. Introduction

The Ti6Al4V titanium alloy combines superior mechanical properties with a low density. Therefore, it enables a significant increase in performance of parts in aerospace applications. However, due to its properties, the Ti6Al4V alloy is classified as difficult to machine material [1]. Beside others, the main properties of this alloy include the tendency to cause abrasive wear, a heat resistance of up to approximately ϑ = 550 °C, a low thermal conductivity of λ = 5.8 W/mK and a low Young's modulus of E = 110 - 140 GPa. This leads to high temperatures in the cutting tool, since the heat cannot dissipate through the chips. Moreover, due to the low Young's modulus, self-exited vibrations can develop. In addition, Ti6Al4V shows a tendency to form build-up edges and chemical reactions with the materials of the cutting tools [2]. Therefore, an increased tool wear occurs during the turning of Ti6Al4V. Temperature-active, self-lubricating coatings deposited by PVD can reduce

© 2021 The Authors. Published by SSRN
This is an open access article under the CC BY-NC-ND license (http://creativecommons.org/licenses/by-nc-nd/4.0/)
Peer review statement: Peer-review under responsibility of the scientific committee of the 21st Machining Innovations Conference for Aerospace Industry 2021.

Electronic copy available at: https://ssrn.com/abstract=3947799

the tool wear in the contact zone. For chromium-aluminum-vanadium-nitride (CrAlVN) coating systems previous studies showed that these coatings form lubricating oxide phases between 700 °C ≤ ϑ ≤ 800 °C based on the ability of transition metal vanadium to form low shear strength oxides at the surface [3]. Additionally, the pin-on-disc (PoD) tests also confirmed the friction reducing effect of CrAlVN coatings against Ti6Al4V [4]. However, as compared to PoD test, the temperature and load profile varies during turning of Ti6Al4V. In PoD tests, lubricating oxide phases may already form during the heating phase before tribological loading. However, in turning, the temperature and lubricating oxide phases develop under tribological loads. Therefore, it can be assumed that the wear development is somewhat different in turning operation. In the present study, the oxidation behavior and the initial tool wear within the first two minutes of turning Ti6Al4V were investigated as a function of the coating chemical composition. In literature, it is stated that lower x_{Al}/x_V-ratios encourage the formation of lubricating oxide phases [5]. Therefore, two CrAlVN coatings with different x_{Al}/x_V-ratios were deposited on cemented carbide inserts by a dcMS/HPPMS hybrid process. To better evaluate the effect of the x_{Al}/x_V-ratio on the oxidation behavior, the x_{Al}/x_{Cr}-ratio was kept constant. Subsequently, cutting tests in defined cutting intervals were carried out with the CrAlVN coated cutting tools as well as uncoated reference tools using a CNC lathe. Finally, the tool wear development and geometry changes as a result of the tool workpiece interaction were measured using confocal laser scanning microscopy (CLSM) and scanning electron microscopy (SEM). In order to observe the formation of lubricating oxide phases during Ti6Al4V turning Raman spectroscopy was used to conduct the phase analysis. Raman spectroscopy is particularly suitable for phase measurements on complex shaped cutting tools due to the precise positioning.

2. Experimental details

2.1 Cutting tools

The investigations were conducted using coated and uncoated cemented carbide cutting inserts CNGP 120408 of grade HW-K10, Kennametal Deutschland GmbH, Rosbach, Germany. The tools had a corner radius of $r_\varepsilon = 0.8$ mm, an effective rake angle of $\gamma_{eff} = 2°$, an effective clearance angle of $\alpha_{eff} = 6°$ and a cutting-edge radius of $r_\beta = (6+2)$ µm. The geometry of the tool is shown in Fig. 1.

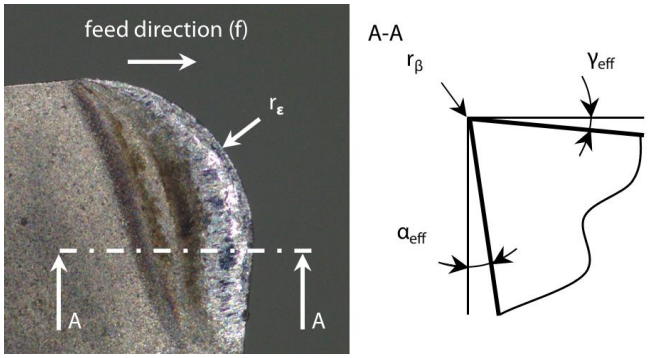

Fig. 1. Geometry of cemented carbide cutting insert CNGP 120408

2.2 Coating deposition

The coatings were deposited using an industrial coating unit CC800/9 HPPMS, CemeCon AG, Würselen, Germany. The coating unit is equipped with two HPPMS cathodes and four dcMS cathodes, see Fig. 2 (a).

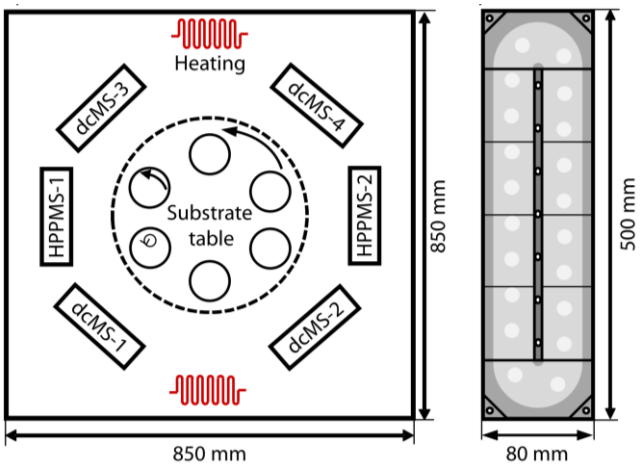

Fig. 2. (a) Schematic representation of coating unit CemeCon CC800/9 HPPMS; (b) schematic representation of a target with 20 plugs.

The targets with a size of A = 500 mm x 88 mm were installed at cathodes to provide the material for the coating deposition. The target material had a purity of 99.9 % for Cr and V and 99.5 % for Al. For deposition of both coatings, CrAlVN-1 and CrAlVN-2, same targets with different cathode powers were used. Table 1 shows the used targets and process parameters. The CrAl20 and VAl20 targets consisted of 20 Al plugs with a diameter d = 15 mm (Fig. 2 (b)).

Table 1. Process parameters for coating deposition

Process parameters	CrAlVN-1 ID-3978	CrAlVN-2 ID-3981
Total pressure p [mPa]	560	560
Argon flow j(Ar) [sccm]	200	200
Nitrogen flow j(N_2) [sccm]	Pressure controlled	Pressure controlled
Heating power P_H [kW]	8.0	8.0
Bias voltage U_{Bias} [V]	-100	-100
HPPMS 1/2 - target / power $P_{HPPMS1/2}$ [kW]	CrAl20 /5.0	CrAl20 /5.0
dcMS-1 - target / power P_{dcMS-1} [kW]	CrAl20 / 4.0	CrAl20 / 4.0
dcMS-2 - target / power P_{dcMS-2} [kW]	V / 2.0	V / 4.5
dcMS-3 - target / power P_{dcMS-3} [kW]	V / 2.0	V / 4.5
dcMS-4 - target / power P_{dcMS-4} [kW]	VAl20 / 4.5	VAl20 / 4.5

Fig. 3 shows a schematic representation of the CrAlVN-1 and CrAlVN-2 coating architecture. For both variants, the coating architecture is identical and only the chemical composition of the self-lubricating functional layer has been changed. A CrAl / CrAlN interlayer was deposited using both HPPMS cathodes solely. The deposition of the self-lubricating functional layer was performed using all six cathodes. During

Electronic copy available at: https://ssrn.com/abstract=3947799

deposition, the cutting tools were arranged in a threefold rotation to gain a homogeneous coating thickness on the cemented carbide inserts.

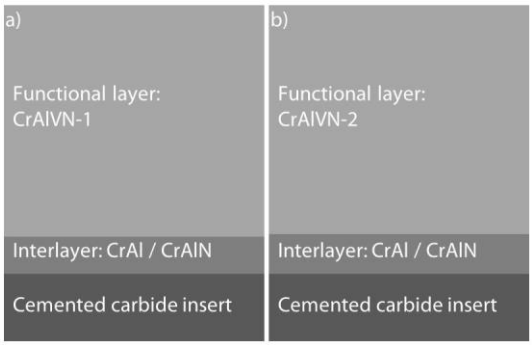

Fig. 3. Schematic representation of the coating architecture of CrAlVN-1 (a) and CrAlVN-2 (b)

2.3 Methods for coating characterization

The coating morphology was determined by SEM. A ZEISS DSM 982 Gemini SEM, Jena, Germany, was used for this purpose. The chemical composition of the coatings was analyzed by electron probe microanalysis (EPMA) using a JEOL LXA-8530, Jeol, Tokyo, Japan. The SEM and EPMA analyses were conducted at the Central Facility for Electron Microscopy (GFE) of RWTH Aachen University. Adhesion between the coating and the cutting inserts was evaluated by Rockwell indentation tests according to DIN 4856. During the test, a Rockwell tip indented the surface perpendicularly with a normal force of $F \approx 588{,}4$ N ($F = 60$ kp). A Rockwell tester HP100, KNUTH Machine Tools GmbH, Wasbek, Germany, was used for this purpose. The indentation region was investigated by CLSM, VK-X 210, Keyence Corporation, Osaka, Japan, to evaluate the adhesive strength category.

2.4 Cutting tests

The cutting tests were conducted using a CNC lathe MD5S, Gildemeister Drehmaschinen GmbH, Bielefeld, Germany, equipped with a dynamometer type 9257B, Kistler Instrumente GmbH, Sindelfingen Germany, for force measurement. The cutting parameters during the longitudinal turning of Ti6Al4V were defined to apply a high thermal load on the tool without the formation of continuous snarling chips. For that a cutting depth of $a_p = 1.2$ mm, a feed rate of $f = 0.12$ mm, a setting angle of $\kappa_r = 95°$ and a cutting velocity of $v_c = 80$ m/min were chosen based on previous wear tests. The tests were conducted in defined cutting intervals of $t_c = 5$ s, 10 s, 20 s, 40 s, 80 s and 120 s. After each interval, a new cutting edge was used to investigate the wear development. Each test was carried out three times using a new cutting edge each time. Due to the high thermal tool load and a significant increase in tool life [6] the cutting tests to determine the wear development and oxidation behavior were carried out using coolant emulsion (9 %) of lubricant B-Cool 675 from Blaser Swisslube AG, Hasle bei Burgdorf, Switzerland. Furthermore, additional cutting tests were carried out under dry cutting conditions. An infrared camera thermoIMAGER TIM 400, Micro-Epsilon, Aachen, Germany, was used to monitor the cutting temperature ϑ_c on the bottom side of the chip directly after leaving the cutting zone, Fig. 4. It can be assumed that the chip temperature at this position immediately after leaving the contact zone is comparable with the temperatures occurring in the contact zone between cutting edge and workpiece [7]. By selecting small measuring ranges in the camera image, the measuring range can be positioned specifically on the underside of the chip. The cutting temperature ϑ_c in each interval was determined at $t_c = (3\pm1)$ s under similar operating conditions after the start of the respective cutting interval. However, the specification of absolute cutting temperatures was not possible for current investigation as reference measurements with a second measurement system were not feasible for the tested coating variants. Measurement of absolute cutting temperatures will be subject of further investigations. Therefore, only temperature differences $\Delta\vartheta$ between both coating variants and the uncoated reference tool were analyzed during current investigation.

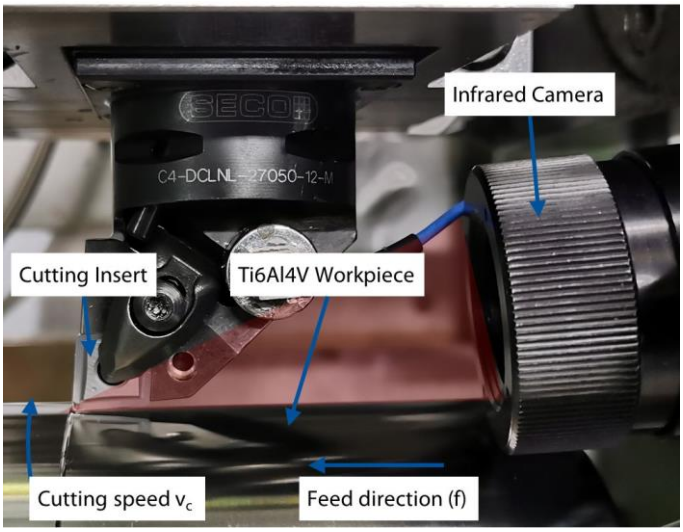

Fig. 4. Experimental setup on CNC lathe Gildemeister MD5S for cutting tests without lubricating coolant

2.5 Methods for wear and oxidation characterization

The oxide phases on the coating surface formed after the cutting intervals were analyzed by Raman spectroscopy. For this purpose, a Raman spectroscope, Renishaw InVia Reflex, Renishaw GmbH, Pliezhausen, Germany, with a $\lambda = 532$ nm laser and a diffraction grating g ($\lambda = 532$ nm) = 1800 l/mm was used. Before each measurement, the laser was calibrated using a silicon reference sample. The measurement parameters were constant for all samples. The wear development on the rake face was measured using the CLSM. Furthermore, the tool wear was investigated by SEM surface images. The chemical composition of the worn surface was determined by means of energy dispersive X-ray spectroscopy (EDS). The nitrogen and oxygen composition were ignored because the weight of these elements is too light for this analysis method. These SEM and EDS analyses were conducted with a Desktop REM Phenom XL, Phenom-World, Eindhoven, Netherlands.

Electronic copy available at: https://ssrn.com/abstract=3947799

3. Results

3.1 Coating characterization

The chemical composition of the coatings was analyzed using ESMA, Table 2. Variation between the chemical composition of the two coatings is due to the difference in the cathode power during the deposition. For coating CrAlVN-2 the x_{Al}/x_V-ratio decreased from $x_{Al}/x_V = 0.5$ to $x_{Al}/x_V = 0.27$. The x_{Al}/x_{Cr}-ratio remained constant at $x_{Al}/x_{Cr} = 0.22$.

Table 2: Chemical composition of the coatings CrAlVN-1 and CrAlVN-2

Coating	x_{Cr}	x_{Al}	x_V	x_N	x_{Al}/x_V	x_{Al}/x_{Cr}
CrAlVN-1	28.6	6.4	12.7	52.3	0.50	0.22
CrAlVN-2	23.6	5.3	19.8	51.3	0.27	0.22

The SEM cross-section images indicate almost no differences in morphology of both coatings. The coatings show a fine-columnar microstructure, Fig. 5. Fine-columnar microstructures are typical for hybrid processes with a comparatively high dcMS-proportion [8]. Therefore, an influence on the wear behavior due to a difference in coating morphology can be neglected.

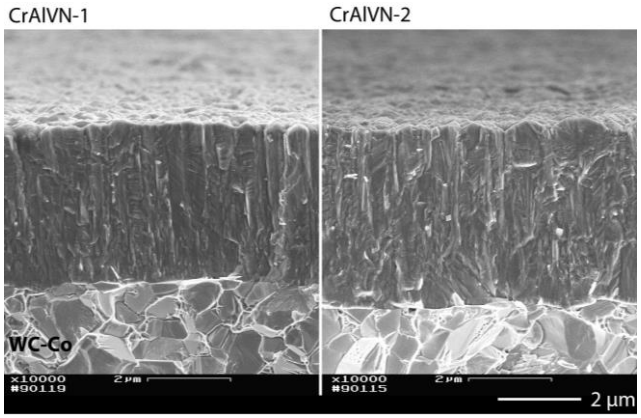

Fig. 5. SEM cross-section images of CrAlN-1 and CrAlN-2 deposited on cemented carbide

The roughness values Ra and Rz were investigated on the peripherally grinded flank-face of the cutting insert. Due to grinding marks on the surface, directionally dependent roughness values were measured. Therefore, Table 3 shows the surface roughness values Ra and Rz parallel and perpendicular to the grinding marks. Both coatings showed comparable roughness values. It is assumed that the small differences in the roughness values of the coatings have negligible influence on the wear behavior.

Table 3: Roughness values Ra and Rz of the coatings CrAlVN-1 and CrAlVN-2

Roughness value / direction	CrAlVN-1	CrAlVN-2
Rz [µm] / parallel	0.14	0.15
Rz [µm] / perpendicular	0.67	0.85
Ra [µm] / parallel	0.02	0.02
Ra [µm] / perpendicular	0.09	0.11

To investigate the adhesion between the coatings and the cemented carbide substrate, Rockwell indentation tests were carried out. Fig. 6 shows CLSM micrographs of these tests on the coated cemented carbide turning tools. Except the orthogonal cracks no coating spallation was detected inside the indentation imprint or on the edge area. Therefore, the adhesion strength of both coatings on the carbide cuttings tool is classified as HF 1.

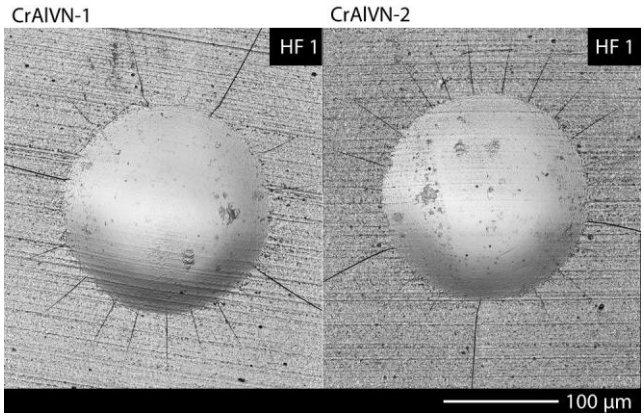

Fig. 6: CLSM micrographs of Rockwell indents of CrAlN-1 and CrAlN-2 on cemented carbide tools

3.2 Wear characterization

The SEM images of the tool rake face after a cutting time of $t_c = 5$ s and $t_c = 120$ s are shown in Fig. 7. As compared to the tool wear after $t_c = 5$ s, Fig. 7 a),c),e), a significant increase is seen after $t_c = 120$ s, Fig. 7 b),d),f) for all variants. When considering the dark area below the cutting edge, a difference between the coated and the uncoated tools is apparent. Already after a cutting time of $t_c = 5$ s, the dark area on the uncoated cutting tool, Fig. 7 e), is more pronounced compared to the coated variants. After a cutting time of $t_c = 120$ s, the dark area on the uncoated tool is still the most pronounced one, Fig. 7 f). The size of the dark areas on the coated variants is almost similar. Further analysis showed that a groove is present in the dark area. Accordingly, this groove can be interpreted as crater wear. Nevertheless, the dark area is presumably not only caused by a reduced image resolution at the groove, but also by element contrast due to chemical reactions.

The white marked rectangle in Fig. 7 a) marks the position at which the detailed images of the rake faces were taken for all cutting tests. The images were examined for break outs and

Electronic copy available at: https://ssrn.com/abstract=3947799

chipping at the cutting edge. Furthermore, EDS measurements were carried out to identify areas of adhesive wear.

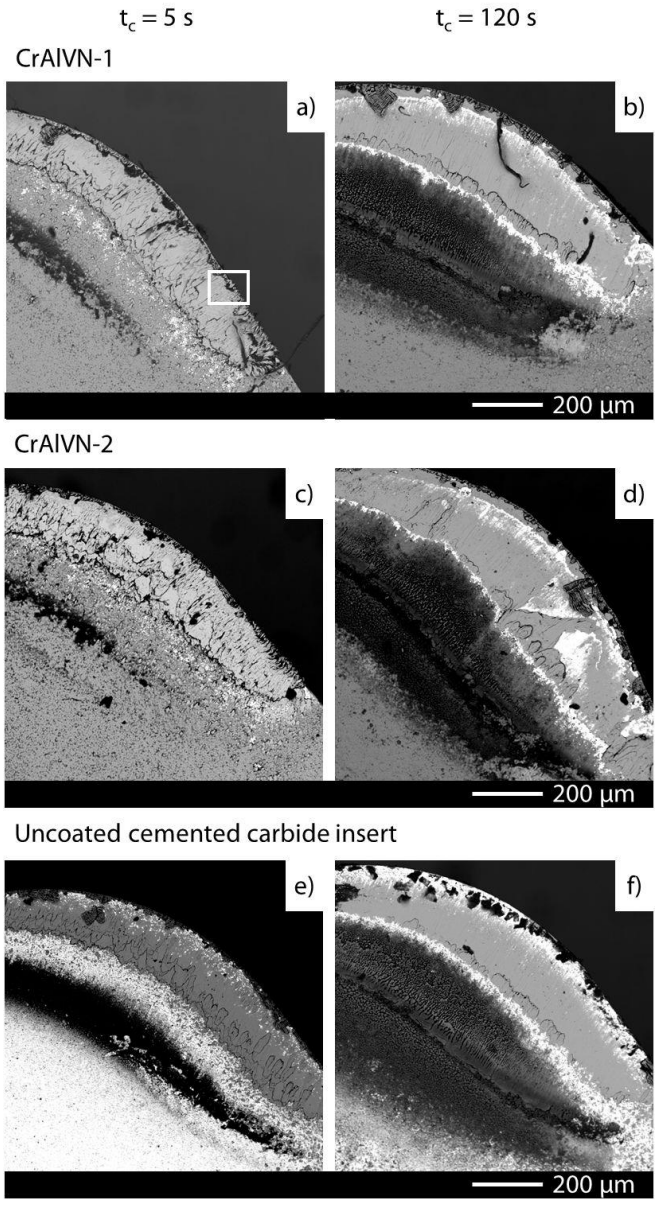

Fig. 7. SEM images of the rake face after the cutting interval t_c = 5 s and t_c = 120 s

Fig. 8 shows the wear development in CrAlVN-1 on the rake face. An excessive adhesion of the counterpart material Ti6Al4V took place on the rake face after a cutting time of t_c = 5 s, Fig. 8 a). Moreover, chips were visible directly at the cutting edge after t_c = 10 s, Fig. 8 b. Fig. 8 c) indicates that the number of Ti6Al4V adhesive debris decreased at t_c = 20 s. The EDS measurements confirmed the presence of coating material next to the cutting edge at t_c = ??. This indicates that the coating survived the strong Ti6Al4V adhesion at the very beginning of the cutting process. The eventual reduction of the Ti6Al4V debris might indicate that the oxidation processes occurring at the cutting edge led to a lower coefficient of friction (COF). With further increase in cutting time t_c, the number of white areas increased, Fig. 8 e), f). These areas, mainly represent tungsten as detected by EDS. Moreover, despite the detected adhesions and chipping at t_c = 120 s, the coating material was still intact as confirmed by EDS measurements.

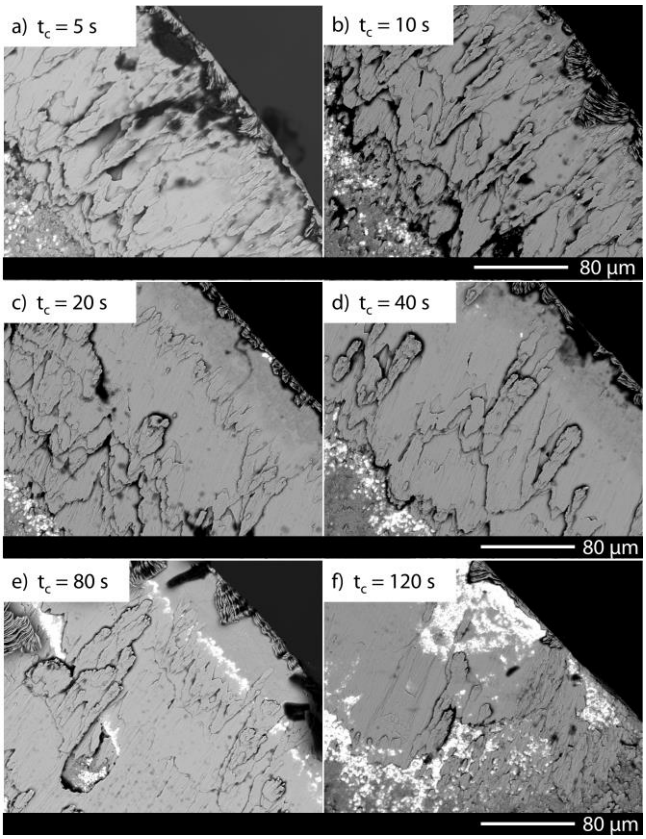

Fig. 8. Detailed SEM images of the wear phenomena on the rake face of the cutting tools coated with CrAlVN-1

Due to the excessive adhesion of Ti6Al4V on the rake face, the formed oxide phases were analyzed on the tool flank face near the cutting edge by Raman spectroscopy. The aim was to investigate the formation of lubricating oxide phases near the cutting edge under cooling lubricant. The black graph shows the spectrum of the coating CrAlVN-1 in the "as-deposited" state. Only one peak which can be attributed to $CrVO_4$ [9], was detected. Peaks which indicate strong oxidation of aluminum or vanadium were not detected. The blue graph shows the Raman spectrum after a cutting time of t_c = 10 s. The spectrum shows various peaks which can be assigned to different oxide phases such as $CrVO_4$ [9], $AlVO_4$ [10], V_2O_5 [9, 11] and the formation pattern V_nO_{2n-1} [11]. In addition, some peaks are attributed to TiO_2 [13] resulting from the adhesion of the workpiece material Ti6Al4V. In literature, V_2O_5 as well as oxides according to the formation pattern V_nO_{2n-1} are considered as lubricating oxide phases [12]. This is attributed to the easily shearable lattice structure of these oxide phases. Moreover, V_2O_5 has relatively low melting point of T_M = 690 °C. If this temperature is exceeded during cutting, a lubricating oxide film can form on the surface. This can contribute to the friction reduction and lead to a more homogeneous cutting force distribution. After a cutting time of t_c = 80 s, hardly any change in the spectrum is detectable. Therefore, it is assumed that the oxidation processes remain unchanged at higher cutting times.

Electronic copy available at: https://ssrn.com/abstract=3947799

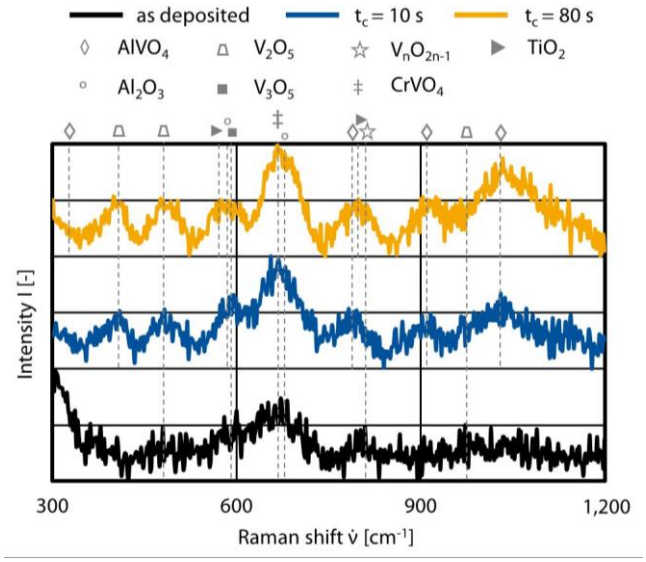

Fig. 9. Raman spectra at the tool flank surface of CrAlVN-1 after the cutting intervals t_c = 10 s and t_c = 80 s

The SEM images of the wear development in the tools coated with CrAlVN-2 are shown in Fig. 10. Compared to the coating system CrAlN-1, no significant changes in the wear mechanisms were found.

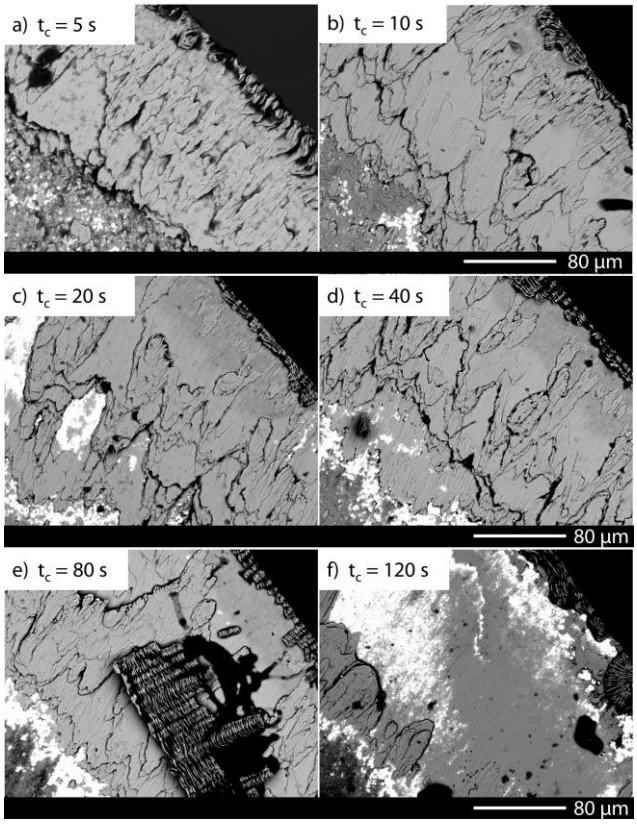

Fig. 10. Detailed SEM images of the wear phenomena on the rake face of the cutting tools coated with CrAlVN-2 after the cutting intervals

However, detailed investigations show that relatively large white areas after a cutting time of t_c = 20 s are present, see Fig. 10 c). The EDS analysis of these areas revealed that substrate was exposed. Presumably, the coating was ripped off by shearing process of the Ti6Al4V adhesions. In Fig. 10 e), a part of a chip which adhered to the surface is visible. At t_c = 120 s, large parts of the coating within a distance of d = 160 µm seems to be removed, Fig. 10 f. Nevertheless, behind this area, the coating is still undamaged. The tool flank surface of CrAlVN-2 was additionally analyzed by Raman spectroscopy, Fig. 11.

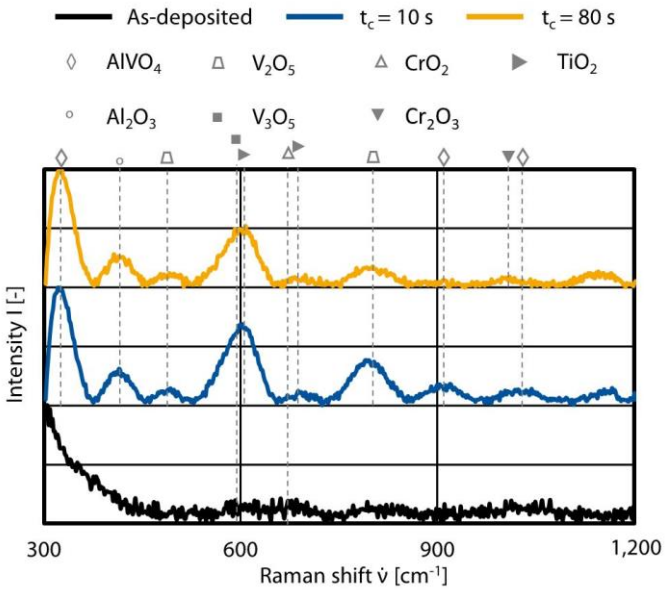

Fig. 11. Raman spectra at the tool flank surface of CrAlVN-2 after the cutting intervals t_c = 10 s and t_c = 80 s

For the coating CrAlVN-2, the Raman spectra before the cutting tests is shown as a black graph. It shows no significant peaks which can be attributed to coating oxidation. After a cutting time t_c = 10 s, several oxide peaks are visible which can be assigned to the oxides Cr_2O_3 [14], $AlVO_4$, V_3O_5 [11], V_2O_5 and TiO_2. After the cutting time of t_c = 10 s, CrAlVN-2 shows more pronounced V_2O_5 oxide peaks compared to the CrAlVN-1 coating. Therefore, a higher tendency to form vanadium oxides can be assumed for CrAlVN-2 based on the lower x_{Al}/x_V ratio. In [15], it was shown for other coating systems that reduced x_{Al}/x_V ratios lead to a stronger formation of vanadium oxides. However, in present case, the intensity of the oxidation seems to decrease at t_c = 80 s. This might be the result of a very fast oxidation process in the beginning followed by wear process.

Fig. 12 shows the wear behavior of the uncoated reference tools. It should be noted that the adhesions at t_c = 5 s, Fig. 12 a), are initially lower compared to the coated tools. The amount of these adhesions increases until a cutting time of t_c = 40 s, Fig. 12 d). On the other hand, for the CrAlVN-1 and CrAlVN-2 coated variants, a tendency towards decreased adhesions can be observed after comparable periods of cutting times. In addition, until the cutting interval t_c = 40 s, the uncoated variant shows a more pronounced adhesion of chip residues directly at the cutting edge. At t_c = 80 s, Fig. 12 e) a uniform film of the workpiece material Ti6Al4V formed near the cutting edge, which is visible as light grey film. Moreover, at t_c = 120 s, Fig. 12 f), small dark areas directly at the cutting edge are detectable. In those areas the carbide substrate seems

Electronic copy available at: https://ssrn.com/abstract=3947799

to be weakened, which can possibly promote an early tool failure.

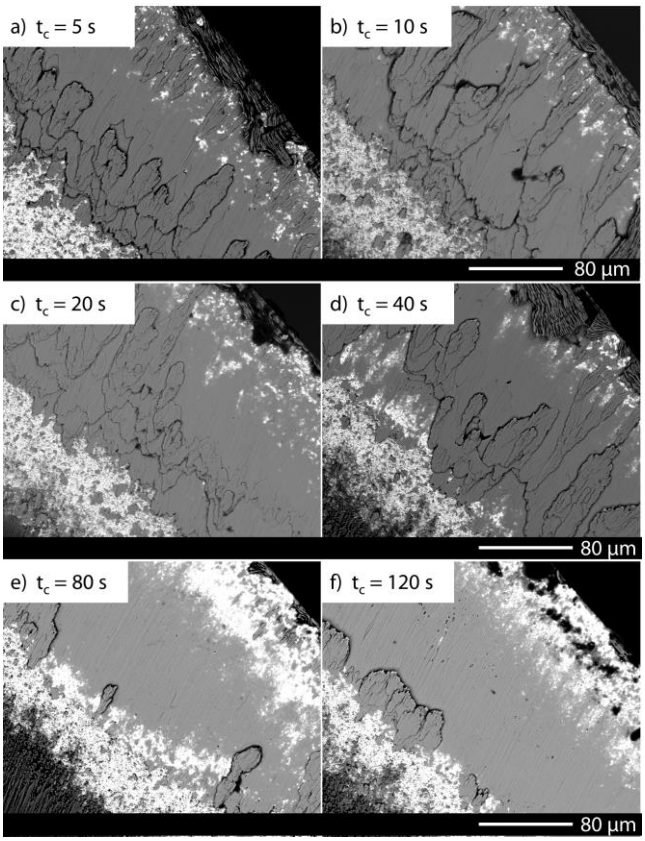

Fig. 12.Detailed SEM images of the wear phenomena on the rake face of the uncoated cutting tools after the cutting intervals

Fig. 13 shows the Raman spectra corresponding to the tool flank surface of the uncoated reference tools. The black graph shows the initial state with a strong peak of CoO [16] and a smaller peak of WO_3 [17]. After a cutting time of t_c = 10 s, small oxide peaks are present in the Raman spectrum. Most of them can be assigned to the oxides $AlVO_4$, TiO_2, and V_2O_5. Although these elements are not present in the cemented carbide substrate, the workpiece material Ti6Al4V contains these elements. Therefore, it can be concluded that the Ti6Al4V adhesions are oxidized due to the high cutting temperatures. The Raman spectra shows, that the oxidation is sustained even after a cutting time of t_c = 80 s. Moreover, for both cutting times, a peak which can be attributed to PO_4- [18] occurred which can be attributed to interactions with the cooling lubricant. Nevertheless, the amount of vanadium oxide peaks of the uncoated reference tools are lower compared to the peaks of the coatings CrAlVN-1 and CrAlVN-2.

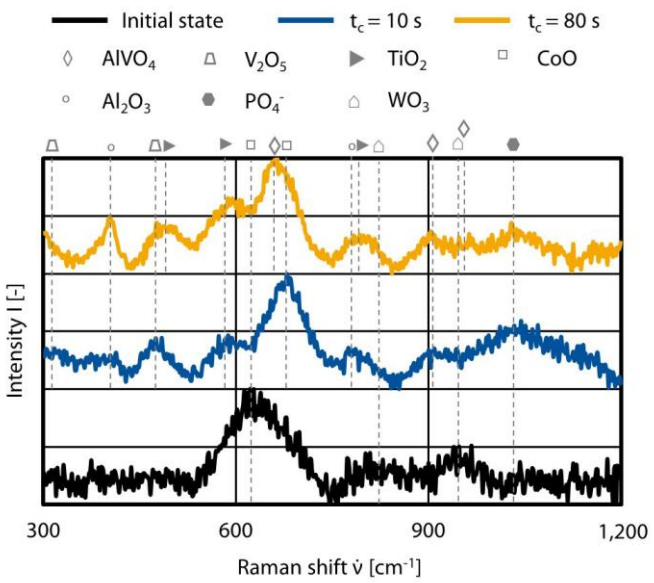

Fig. 13. Raman spectra at the tool flank surface of the uncoated reference tool after the cutting intervals t_c = 10 s and t_c = 80 s

Since the conducted cutting tests did not show significant differences in the cutting forces between the coatings, this will not be discussed further. In order to investigate the effects of the coatings on the temperature present in the contact zone, an infrared camera was used to measure them under dry cutting conditions. Subsequently, the prevailing temperatures on the underside of the chip after t_c = (3±1) s near the chip forming area were evaluated. Since the measurement conditions were not suitable to specify absolute temperatures, only temperature differences between the coated variants were compared with each other. These are shown in Fig. 14.

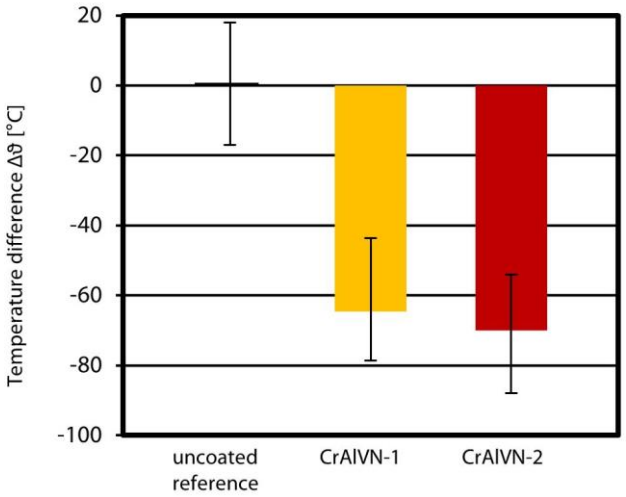

Fig. 14. Temperature differences Δϑ determined between the uncoated reference tools and the coating variants CrAlVN-1 and CrAlVN-2 after cutting time t_c = (3±1) s.

The reference temperature measurements for the uncoated variants were assigned a level zero. Based on that, an average temperature difference of approximately $\Delta\vartheta \approx -64$ °C was determined for coating CrAlVN-1. For CrAlVN-2, a slightly increased average temperature difference of approximately

Electronic copy available at: https://ssrn.com/abstract=3947799

$\Delta\vartheta \approx 70$ °C was observed. Such temperature differences could be attributed to the reduced friction due to the formation of lubricating oxide phases. The Raman spectra shown in Fig. 9 and Fig. 11 indicate slight differences in formation of lubricating oxide phases such as V_2O_5 which are more pronounced for the coating CrAlVN-2. This correlates with the measured temperature differences and therefore supports the assumption regarding the influence of lubricating oxide phases on the cutting conditions. In general, a reduction of the cutting temperature can lead to an increased substrate protection to prevent premature tool failure.

4. Conclusion

Self-lubricating coatings are suitable for friction reduction in high temperature machining processes of Ti6Al4V. The investigation on the wear behavior of the cutting tool during the turning of Ti6Al4V under flood cooling within a maximum cutting time of $t_c = 120$ s showed following findings:

- Strong adhesions of Ti6Al4V and the formation of build-up edges were the main causes of tool wear for all variants. Nevertheless, the CrAlVN-2 coating showed a tendency towards an earlier reduction of adhesion processes compared to the uncoated reference.
- Raman investigations showed the formation of lubricating vanadium oxides in turning while using cooling lubricant. The strongest trend for these oxide phases were detected for the CrAlVN-2 coating system. Thus, it can be assumed that the use of self-lubricating coating systems is suitable for turning operations in wet cutting conditions. Moreover, such coatings offer a great potential to increase tool life.
- The observed temperature differences between the uncoated reference tool and the coated variants supports the assumption that the formation of lubricating oxide phases have a positive effect on the friction behavior at the tribological contact area between the tool and workpiece.

The investigation showed that the chemical composition of the CrAlVN coating needs to be adapted in order to reduce the adhesion processes during the turning of workpiece material Ti6Al4V. Therefore, the adaptation of the chemical composition of the CrAlVN coatings for machining applications will be the subject of further research.

Acknowledgements

The authors gratefully acknowledge the financial support of the German Research Foundation, Deutsche Forschungs-gemeinschaft (DFG) within the research project “Unter-suchung temperaturaktiver, reibungsmindernder Schicht-systeme für die Drehbearbeitung von Titanlegierungen”, BO 1979/69-1 / HI 843/10-1, with the project number 422345568.

References

[1] Klocke, F. Zerspanung mit geometrisch bestimmter Schneide. 9th ed. Berlin: Springer Vieweg; 2018.
[2] Kramer, B. M., Viens, D., Chin, S. Theoretical Consideration of Rare Earth Metal Compounds as Tool Materials for Titanium Machining. CIRP Annals 1993; 42:111–114.
[3] H. Czichos, K.-H. Habig (Eds.). Tribologie-Handbuch: Tribometrie, Tribomaterialien, Tribotechnik. 4th ed. Wiesbaden: Springer Vieweg; 2015.
[4] Brugnara, R.H. Hochtemperaturaktive HPPMS-Verschleißschutzschichten durch Bildung reibmindernder Magnéli-Phasen im System (Cr,Al,X)N. Dissertation 2015.
[5] Franz, R., Mitterer, C. Vanadium containing self-adaptive low-friction hard coatings for high-temperature applications: A review. Surface and Coatings Technology 2013; 228:1–13.
[6] Krämer, A., Klocke, F., Sangermann, H., Lung, D. Influence of the lubricoolant strategy on thermo-mechanical tool load, CIRP J Manuf Sci Technol 2014; 7 40-47
[7] Lenz, E. Die Temperaturmessung in der Kontaktzone Span- Werkzeug beim Drehvorgang. Annals of the CIRP 1965;201.
[8] Bobzin, K., Brögelmann, T., Kruppe, N.C., Engels, M. Influence of HPPMS on Hybrid dcMS/HPPMS (Cr,Al)N Processes, Surf. Coat. Technol. 2019, 358 57-66
[9] Tian, H., Wachs, I. E., Briand, L. E. Comparison of UV and visible Raman spectroscopy of bulk metal molybdate and metal vanadate catalysts. The journal of physical chemistry. B 2005; 109 23491–23499.
[10] Barshilia, H. C., Rajam, K. S. Raman spectroscopy studies on the thermal stability of TiN, CrN, TiAlN coatings and nanolayered TiN/CrN, TiAlN/CrN multilayer coatings. J. Mater. Res 2004; 19 3196–3205.
[11] Shvets, P., Dikaya, O., Maksimova, K., Goikhman, A. A review of Raman spectroscopy of vanadium oxides. J Raman Spectrosc 2019; 50 1226–1244.
[12] Erdemir, A. A crystal chemical approach to the formulation of self-lubricating nanocomposite coatings. Surface and Coatings Technology 2005; 200 1792–1796.
[13] Tompsett, G. A., Bowmaker, G. A., Cooney, R. P., Metson, J. B., Rodgers, K. A., Seakins, J. M.: The Raman spectrum of brookite, TiO2 (Pbca, Z = 8). J Raman Spectrosc 1995; 26 57–62.
[14] Sánchez-López, J. C., Contreras, A., Domínguez-Meister, S., García-Luis, A., Brizuela, M. Tribological behaviour at high temperature of hard CrAlN coatings doped with Y or Zr. Thin Solid Films 2014; 550 413–420.
[15] Zhou, Z., Rainforth, W. M., Rodenburg, C., Hyatt, N. C., Lewis, D. B., Hovsepian, P. E. Oxidation Behavior and Mechanisms of TiAlN/VN Coatings. Metall and Mat Trans A 2007; 38 2464–2478.
[16] Bouzourâa, M.-B., Rahmani, M., Zaïbi, M.-A., Lorrain, N., Hajji, L., Oueslati, M. Optical study of annealed cobalt–porous silicon nanocomposites. Journal of Luminescence 2013; 143 521–525.
[17] Martin, C., Hijazi, H., Addab, Y., Domenichini, B., Bannister, M. E., Meyer, F. W., Pardanaud, C., Giacometti, G., Cabié, M., Roubin, P. Tungsten oxide thin film bombarded with a low energy He ion beam: evidence for a reduced erosion and W enrichment. Phys. Scr 2017; T170 14019.
[18] Markevich, E., Sharabi, R., Haik, O., Borgel, V., Salitra, G., Aurbach, D., Semrau, G., Schmidt, M. A., Schall, N., Stinner, C. Raman spectroscopy of carbon-coated LiCoPO4 and LiFePO4 olivines. Journal of Power Sources 2011; 196 6433–6439.

Electronic copy available at: https://ssrn.com/abstract=3947799